The Role of Sulfur Dioxide in Stratospheric Aerosol Formation Evaluated Using In-Situ Measurements in the Tropical Lower Stratosphere

A. W. Rollins[1,2], T. D. Thornberry[1,2], L. A. Watts[1,2], P. Yu[1,2], K. H. Rosenlof[2], M. Mills[3], E. Baumann[4], F. R. Giorgetta[4], T. V. Bui[5], M. Höpfner[6], K. A. Walker[7,8], C. Boone[8], P. F. Bernath[8,9], P. R. Colarco[10], P. A. Newman[10], D. W. Fahey[1,2], and R. S. Gao[2]

[1]Cooperative Institute for Research in Environmental Sciences, Boulder, CO, USA.

[2]NOAA Earth System Research Laboratory, Chemical Sciences Division, Boulder, CO, USA.

[3]National Center for Atmospheric Research, Boulder, CO, USA

[4]National Institute of Standards and Technology, Boulder, CO, USA

[5]NASA Ames Research Center, Moffett Field, CA, USA

[6]Institute of Meteorology and Climate Research, Karlsruhe Institute of Technology, Karlsruhe, Germany

[7]Department of Physics, University of Toronto, Toronto, ON, Canada

[8]Department of Chemistry, University of Waterloo, Waterloo, ON, Canada

[9]Department of Chemistry and Biochemistry, Old Dominion University, Norfolk, VA, USA

[10]NASA Goddard Space Flight Center, Greenbelt, MD, USA

Corresponding author: Andrew Rollins (andrew.rollins@noaa.gov)

Key Points:

- First in-situ measurements of SO_2 in the tropical UT/LS.
- Typical SO_2 at the tropical tropopause is near 5-10 pptv.
- Flux of SO_2 across the tropopause is likely to be a minor source of stratospheric aerosol.

Abstract

Stratospheric aerosols (SAs) are a variable component of the Earth's albedo that may be intentionally enhanced in the future to offset greenhouse gases (geoengineering). The role of tropospheric-sourced sulfur dioxide (SO_2) in maintaining background SAs has been debated for decades without in-situ measurements of SO_2 at the tropical tropopause to inform this issue. Here we clarify the role of SO_2 in maintaining SAs by using new in-situ SO_2 measurements to evaluate climate models and satellite retrievals. We then use the observed tropical tropopause SO_2 mixing ratios to estimate the global flux of SO_2 across the tropical tropopause. These analyses show that the tropopause background SO_2 is about 5 times smaller than reported by the average satellite observations that have been used recently to test atmospheric models. This shifts the view of SO_2 as a dominant source of SAs to a near-negligible one, possibly revealing a significant gap in the SA budget.

1 Introduction

Stratospheric aerosols (SAs) are an important component of the Earth's radiative balance. Because SA lifetimes are on the order of 100 times those of tropospheric aerosols [*Crutzen*, 2006], the relatively small sources of SAs are disproportionally significant for climate. SAs also provide surfaces for catalytic chemistry that can efficiently destroy stratospheric ozone [*Solomon*, 1999]. A number of proposals suggest that it may become necessary to attempt to mitigate global warming (i.e. climate intervention (CI), solar radiation management, or geoengineering) by enhancing SAs through direct injection of sulfur dioxide gas (SO_2) into the lower stratosphere [*Shepherd*, 2012; *McNutt et al.*, 2015]. For all of these reasons the chemistry and source gases that control the SA burden in both current and future climates are of wide interest.

Filter measurements [*Junge et al.*, 1961], volatility measurements [*Rosen*, 1971; *Borrmann et al.*, 2010], and mass spectrometer measurements [*Arnold et al.*, 1998; *Murphy et al.*, 2014] all point to SA being dominated by sulfuric acid (H_2SO_4)-water mixtures, although recent work has shown that in the upper troposphere and lower stratosphere (UT/LS) organic material may sometimes be a significant fraction of the mass [*Brühl et al.*, 2012; *Murphy et al.*, 2014; *Yu et al.*, 2016]. *Crutzen* [1976] originally proposed that oxidation of carbonyl sulfide (COS) to form H_2SO_4 might play a dominant role as a source of SAs because of its ubiquitous tropospheric mixing ratio of ~500 pptv, and its efficient photolytic destruction in the stratosphere. While subsequent modeling studies have agreed that COS plays an important role [*Chin and Davis*, 1995; *Thomason and Peter*, 2006; *Brühl et al.*, 2012; *Sheng et al.*, 2015], the fraction of the SA burden that can explained by COS oxidation during volcanically quiescent periods remains unclear.

Other than COS, the only gas-phase stratospheric sulfur source that is thought to potentially be a major term in the background SA budget is SO_2. Because SO_2 is completely converted to H_2SO_4 and then SA on a time scale of ~ 1 month in the lower stratosphere, the flux of SO_2 into the stratosphere can be considered to be an equivalent source of sulfate aerosol. With the current global anthropogenic emission of SO_2 near 60,000 GgS yr^{-1} [*Smith et al.*, 2011], even a very small fraction entering the stratosphere would be significant compared with the approximately 100 GgS yr^{-1} estimated as necessary to maintain the SA burden. Recent positive trends in SA

have been suggested to potentially result from increased anthropogenic emissions, particularly in Asia where the summer Asian monsoon anticyclone efficiently transports pollutants including SO_2 to the lower stratosphere [*Hofmann et al.*, 2009; *Randel et al.*, 2010]. Others have shown that the apparent trend can be mostly explained by a series of minor volcanic eruptions [*Vernier et al.*, 2011; *Neely et al.*, 2013; *Brühl et al.*, 2015; *Mills et al.*, 2016]. In-situ measurements of SO_2 at the tropical tropopause where the majority of species enter the stratosphere have however not previously been available, and this has long been recognized as leaving significant uncertainty in the relative importance of this stratospheric sulfur source [*Kremser et al.*, 2016]. Unlike COS, SO_2 processes in the troposphere are complex. A large suite of natural and anthropogenic SO_2 point sources and the SO_2 reactivity with hydroxyl radicals (OH) and oxidants dissolved in cloud droplets result in a heterogeneous SO_2 distribution in the UT. Transport into the UT through deep convection is particularly uncertain due to the sensitivity of aqueous-phase sulfur oxidation chemistry to parameters such as pH and the availability of hydrogen peroxide. Therefore, having confidence in modeled UT/LS SO_2 abundances requires direct validation.

To understand the tropospheric SO_2 contribution to the SA budget, we performed the first in-situ SO_2 measurements at and above the tropopause in the tropics. Here we present these measurements and compare the in-situ measurements to calculations using two chemistry-climate models. We then use the models as a form of transfer standard to evaluate the accuracy of the retrievals of background SO_2 mixing ratios from the MIPAS satellite instrument (Michelson Interferometer for Passive Atmospheric Sounding) [*Höpfner et al.*, 2013, 2015], as well as those from the ACE-FTS satellite instrument (Atmospheric Chemistry Experiment – Fourier Transform Spectrometer) [*Doeringer et al.*, 2012]. Finally, we provide an estimate of the global annual flux of SO_2 into the stratosphere, and discuss its contribution to the SA budget.

2 Methods

2.1 In-situ measurements

An in-situ instrument based on a laser-induced fluorescence (LIF) technique was used in this study to achieve the desired sensitivity for SO_2 mixing ratios on the order of 1 part per trillion (pptv, 10^{-12} number mixing ratio) and to afford operation onboard the NASA WB-57F high-altitude research aircraft [*Rollins et al.*, 2016]. The instrument excites SO_2 using a tunable laser near 216.9 nm and detects the resulting red-shifted fluorescence at 240 – 400 nm. Typical precision (1σ) during aircraft operation with 10 seconds of integration is 2 pptv. For the present analysis the LIF data were averaged to 1 minute, reducing the uncertainty due to instrument noise to < 1 pptv. Systematic uncertainty in the measurement is ±16% + 0.9 pptv.

During the NASA VIRGAS experiment (Volcano-plume Investigation Readiness and Gas-phase and Aerosol Sulfur) in October 2015, the instrument acquired over 18 h of SO_2 measurements in the UT/LS with flights based from Houston, TX, spanning 10.8 °N – 45.4 °N latitude at altitudes up to 19.4 km (Fig. 1). The in-situ temperature and ozone measurements indicated that the tropopause in the tropical regions during these flights was typically near 17 km (Fig. 2). No large volcanic eruptions are known to have occurred immediately prior to or during the sampling

period that might have significantly affected our measurements. A number of effusive volcanoes in Mexico and Central America however were active during that time, and some isolated plumes that were encountered in the UT can be traced back as likely having originated from those sources.

2.2 CESM1(WACCM)

We conducted detailed calculations of the sulfur budget and transport across the tropopause, using the Community Earth System Model, version 1, (CESM1) with the Whole Atmosphere Community Climate Model (WACCM) [*Marsh et al.*, 2013]. *Mills et al.* [2016] describe the development of the CESM1(WACCM) version used here. Sources of sulfur-bearing gases are included in the model as either time-varying lower boundary conditions, as for dimethyl sulfide (DMS) and OCS, or direct emissions from natural and anthropogenic sources, as for SO_2 from pollution and volcanoes [*Dentener et al.*, 2006]. This includes effusive volcanoes in Mexico and Central America. The model includes a prognostic treatment of aerosols, including sulfate in the troposphere and stratosphere. CESM1(WACCM) is run at 1.9° latitude x 2.5° longitude horizontal resolution, with 88 vertical levels from surface to $6x10^{-6}$ hPa. The vertical resolution near the tropopause is about 1 km. Horizontal winds and temperatures are nudged to specified dynamics (SD) from the Goddard Earth Observing System Model (GEOS-5) using a 50-hour relaxation time. We initialized SD-WACCM for January 1, 2015, with conditions generated by the volcanic simulation described in *Mills et al*. [2016]. We ran SD-WACCM from January 1 to October 31, 2015, including the input of 0.4 Tg SO_2 from the eruption of Calbuco (72.614°W, 41.326°S) on April 23, 2015.

2.3 GEOS-5

During VIRGAS the NASA GEOS-5 model [*Rienecker et al.*, 2007; *Molod et al.*, 2015] provided near-real time (NRT) global forecasts and analyses of meteorological and chemical fields. GEOS-5 comprises an atmospheric general circulation model coupled to a 3DVar data assimilation system for meteorological fields and incorporates assimilation of bias-corrected aerosol optical depth observations from MODIS [*Buchard et al.*, 2015]. The NRT GEOS-5 products (available here: https://gmao.gsfc.nasa.gov/forecasts/) were provided at a global 0.25° latitude x 0.3125° longitude horizontal resolution, with 72 vertical levels from the surface to 0.01 hPa and vertical resolution of about 1 km near the tropopause. The chemistry module used here is based on the Goddard Chemistry, Aerosol, Radiation, and Transport (GOCART) module, as described in *Colarco et al.* [2010], and includes simulation of dust, sea salt, sulfate, and carbonaceous aerosols. SO_2 inputs to the model are derived from anthropogenic and volcanic sources including effusive volcanoes in Mexico and Central America. SO_2 is also produced from oxidation of DMS, and conversion to sulfate occurs in gas phase and aqueous processes using

prescribed oxidant inventories based on the Global Modeling Initiative chemical transport model (GMI) [*Duncan et al.*, 2007; *Strahan et al.*, 2007].

2.4 Satellites

Retrievals of SO_2 volume mixing ratios have been performed using spectra from ACE-FTS [*Doeringer et al.*, 2012] and MIPAS [*Höpfner et al.*, 2013, 2015]. Retrievals of SO_2 are available from ACE-FTS for the time range covering January 2004 until September 2010, and from MIPAS from July 2002 until April 2012. For MIPAS, we use monthly means of the single-radiance SO_2 retrievals (data versions V5R_SO2_20, V5R_SO2_220, V5R_SO2_221) [*Höpfner et al.*, 2015]. While the MIPAS single-radiance retrievals provide global daily coverage, the precision of these data at low SO_2 mixing ratios is 70 – 100 pptv, necessitating significant averaging to quantify background SO_2 in the UT/LS. To compare the satellite retrievals with our in-situ measurements we use zonally averaged satellite profiles from 10 - 25°N during the periods when enhancements due to significant volcanic activity appear to be minor as described in *Höpfner et al.* [2013]. For the profiles in Figure 3, we show the median and interquartile range of the individual ACE-FTS retrievals and of the MIPAS monthly means to provide a measure of the variability of the retrieved SO_2 mixing ratios.

3 Discussion

The temperature and ozone structure observed during the VIRGAS flights indicates that air sampled south of 25°N during VIRGAS is representative of tropical air masses (Fig. 2). Therefore, we use measurements south of 25°N to characterize the tropical SO_2 field. Figure 3 shows statistics of the SO_2 measurements made from the aircraft in the tropical UT/LS region, and compares these with the model calculations (Fig. 3a) and satellite retrievals (Fig. 3b). We show the median and interquartile range for the 1-minute averaged in-situ SO_2 measurements (blue markers and shading). In the lower stratosphere (18 km and above) a narrow distribution centered near 3 pptv was observed, and values above 10 pptv were rare. In the tropopause region (~17 km), a broader distribution was observed with a median value of 10.8 pptv. In the upper troposphere (14-17 km) only a minor vertical gradient is observed, likely evidence of vertical mixing related to the extensive convection in this region.

Figure 3a presents two profiles produced using both the WACCM and GEOS-5 models. For each model an average SO_2 profile is derived by sampling the model along aircraft flight-tracks (Fig. 3a solid lines). In addition, an annual zonal mean profile from each model for 2015 is calculated to estimate typical tropopause SO_2 levels (Fig. 3a and 3b, dashed lines). Because the models include all known volcanoes globally, the zonal average model profiles estimate effects of volcanoes outside of the sampling region. At the tropopause (~17 km), the flight-track sampled models show SO_2 values that are lower than the aircraft observations of 10.8 pptv by 25% (WACCM, 8.1 pptv) and 31% (GEOS-5, 7.5 pptv), although both models are well within the range of the observations (5.4 - 19.5 pptv). The tropopause zonal mean values from both WACCM (5.1 pptv) and GEOS-5 (4.3 pptv) are somewhat lower than the flight-track sampled model SO_2 mixing ratios. We expect that this is due to influence of local emissions from effusive

volcanoes in Mexico and Central America, which were active during this time and were also included by the models.

The differences between the zonal average and flight-track-sampled model outputs suggests that the aircraft measurements are somewhat high relative to the zonal mean values due to spatial and temporal sampling biases. Thus, comparing the zonal means from the models with those from satellite retrievals is arguably the most reliable way to evaluate the consistency of satellite retrievals with the more spatially and temporally limited in-situ observations. The UT/LS model-satellite comparisons in Fig. 3b for non-volcanic periods show strong agreement between models and ACE-FTS, but large overestimates from MIPAS. For example, at the tropopause the WACCM zonal mean (5.1 pptv) is a factor of 4.6 smaller than the MIPAS mean (23.6 pptv). It is important to note that the MIPAS $\pm 2\sigma$ uncertainty range (-7.4 pptv – 54.6 pptv, not shown in Fig. 3, see [*Höpfner et al.*, 2015]) and the variability at shorter time scales do include the WACCM value. As discussed in *Höpfner et al.* [2015], the MIPAS systematic uncertainties are quite significant relative to background SO_2 mixing ratios. In addition, the potential influence of volcanic SO_2 emissions during the MIPAS period (2002 – 2012) that differ from those during 2015 cannot be completely excluded. To further address this issue we sampled WACCM at the times and locations of the individual MIPAS profiles using a WACCM run that includes explosive volcanoes and reproduces the historic SA burden during the MIPAS 2002 – 2012 period (see [*Mills et al.*, 2016]). Figure 3b shows the mean of these WACCM profiles exhibit a slightly higher, but very similar profile to that for 2015. Overall, the in situ/model/satellite comparison suggests that MIPAS mean values are not useful for characterizing background UT/LS SO_2 without considering the full range of stated uncertainty and temporal variability. This is an important conclusion because MIPAS mean values have been used as an absolute point of reference for recent global model simulations in the LS [*Brühl et al.*, 2015; *Sheng et al.*, 2015].

A primary objective surrounding the various measurements of SO_2 in the LS is whether they suggest that the chemical and transport processes controlling SO_2 in this region are understood well enough to have confidence in the role of SO_2 in maintaining SA mass and, ultimately, in SO_2-based geoengineering simulations. For example, the in-situ observations of the SO_2 vertical gradient in the lower stratosphere is consistent with destruction of SO_2 by OH in conjunction with slow ascent. Assuming a lower stratosphere ascent rate of 0.4 mm s^{-1} [*Schoeberl et al.*, 2008], the transit time between 17 km and 18 km is 29 days. The SO_2 lifetime (*e*-folding) in this region due to reaction with OH is estimated to be about 30 days [*Höpfner et al.*, 2015]. Therefore, if the chemistry and dynamics in the LS are well simulated in models, the SO_2 mixing ratio at 18 km should be about 38% of that at 17 km. This fraction is in reasonable agreement with the in-situ measured ratio (33%) and simulated ratios of 50% (both GEOS5 and WACCM). The larger equivalent ratios from MIPAS (70%) and ACE-FTS (80%) are likely due at least in part to insufficient vertical resolution in the satellite retrievals (~3 km).

An estimate of the annual flux of SO_2 into the stratosphere can be derived by taking the product of the annual mass flux across the tropical tropopause and the mean tropical tropopause SO_2 mixing ratio. *Rosenlof and Holton* [1993] calculated a flux through the tropical tropopause (15 °S – 15 °N) of 6.5 x 10^{11} Gg air yr^{-1}. As reasoned above, the modeled zonal mean provides the most representative values of the SO_2 zonal mean mixing ratio in the LS. Assuming a zonally averaged value of 5.1 pptv SO_2 (5.6 x 10^{-12} sulfur mass mixing ratio) at the tropopause, a flux of 3.6 GgS yr^{-1} is derived. In contrast, the SOCOL-AER modeling study [*Sheng et al.*, 2015] shows SO_2 mixing ratios close to those retrieved by MIPAS and calculates a flux of 50.9 GgS yr^{-1} due

to SO_2 alone, which is a factor of 14 times higher than our derived flux. That study shows an average tropical tropopause mixing ratio of about 30 pptv SO_2 at 17 km for September/October/November, which accounts for a factor of about 6 difference relative to our 5.1 pptv. The remaining factor of 2.3 in the flux is likely due to differences in the assumed troposphere/stratosphere exchanges. *Stenke et al.* [2013] show that the tropical water vapor tape recorder produced in the SOCOL version used by *Sheng et al.* (SOCOLv3T31) implies modeled tropical upwelling that is about 1.85 times as fast as that observed by the HALOE satellite, suggesting that the modeled flux through the tropical tropopause is likely high by a similar factor. This may also imply that the SOCOL-AER stratospheric aerosol lifetime is too short due to an overestimated Brewer-Dobson circulation speed. After the differences in tropopause SO_2 and tropical upwelling, the small remaining difference between our flux estimate and the SOCOL-AER flux is likely due to extratropical transport that is neglected in our analysis and uncertainties in the tropical upwelling. Given that SOCOL-AER does not include eruptive volcanic SO_2 sources, and that the continuous emissions at the surface are quite similar to those used in the WACCM and GEOS-5 simulations, this implies that SOCOL-AER brings about 5.9 times (30 pptv / 5.1 pptv) as much of the surface SO_2 to the tropopause.

Many studies have used various techniques to calculate the flux of sulfur into the stratosphere (in the form of sulfate or its precursors) that would be required to maintain the observed stratospheric aerosol burden [*Chin and Davis*, 1995 and references therein; *Thomason and Peter*, 2006; *Brühl et al.*, 2012; *Sheng et al.*, 2015]. These studies typically either estimate the stratospheric aerosol burden and divide this by the estimated lifetime of the aerosols, or derive the required flux by using a more detailed chemical transport model to reproduce the observed aerosol burden. *Sheng et al.* [2015] used SOCOL-AER to calculate an aerosol burden of 109 GgS, and *Mills et al.* [2016] used WACCM to calculate a burden of 138 GgS. These both are in reasonable agreement with the measured burden using the SAGE (Stratospheric Aerosol and Gas Experiment satellite) 4λ technique [*Arfeuille et al.*, 2013] of 115 GgS during the volcanically quiescent 2000 – 2001 period.

While most of the recent estimates of the total sulfur flux (i.e. SO_2 + OCS + DMS + SO_4 + …) derive numbers greater than 100 GgS yr^{-1}, the full range of reported estimates is from 43 GgS yr^{-1} [*Crutzen*, 1976] to 181 GgS yr^{-1} [*Sheng et al.*, 2015]. As a point of reference here we use 181 GgS yr^{-1} which is the most recently reported value and has been adopted in the recent review paper [*Kremser et al.*, 2016]. Comparing 181 GgS yr^{-1} to the SO_2 flux of 3.6 GgS yr^{-1} derived in this work would indicate the direct stratospheric flux of SO_2 is a near-negligible source of SA at ~2% of the budget. If one compares the *Sheng et al*. SO_2 flux estimate of 50.9 GgS yr^{-1} to our in-situ-based estimate of 3.6 GgS yr^{-1}, our estimate would leave 47.3 GgS yr^{-1}, or approximately 26% of the SA mass budget unaccounted for. This gap cannot be made up by increased COS flux both because the uncertainty in the COS contribution is much less than the additional 47.3 GgS yr^{-1} required, and because COS is an aerosol source only above ~ 20 km [*Chin and Davis*, 1995], while SO_2 is a source of aerosol in the 17-20 km region where the majority of the SA mass resides. To maintain agreement with the vertical distribution of SA that has been observed using remote sensing and optical particle counters [*Thomason and Peter*, 2006], a gap in the SA budget could likely be filled by an increased flux of sulfate aerosols, or other aerosols or their precursor gases such as organic compounds, which generally have not been included in SA modeling studies. A second possibility is that the total budget of 181 GgS yr^{-1} is significantly overestimated, which could be due to an underestimate of the SA lifetime. As noted above, this may be the case if SOCOL significantly overestimates the tropical upwelling mass flux. *Brühl et*

al. [2012] for example calculated that about 65 Gg yr^{-1} of OCS (34.7 GgS yr^{-1}) accounts for at 65 – 75 % of the SA source, implying that the total budget is only 46 – 53 GgS yr^{-1}. Clearly, uncertainties in the SA budget still lie in both the rates of exchange between the troposphere and stratosphere, and in the role of spatial and temporal inhomogeneity in SO_2 in the UT. Resolving this issue will require more UT measurements in important convective regions and near regions with unique SO_2 emissions (e.g. Asia).

SO_2-based CI scenarios suggest that a sustained stratospheric input of $10^3 – 10^4$ GgS yr^{-1} would be required to increase the SA burden to sufficiently offset the radiative forcing from a doubling of pre-industrial CO_2 [*McNutt et al.*, 2015]. In such a world, the current budget (~10^2 GgS yr^{-1}) of background SA mass becomes irrelevant. However, understanding the present-day chemistry and dynamics that controls the distribution of aerosols in the stratosphere is the key to predicting the effectiveness and consequences of CI scenarios. An accurate assessment of the vertical distribution of SO_2 in the LS, such as is reported here, helps to provide confidence in the chemistry there, and should be considered an essential benchmark to test models and satellites that might be used to evaluate CI scenarios.

Acknowledgments and Data

This research was funded by the NOAA Atmospheric Chemistry, Carbon Cycle, and Climate Program, and the NASA Radiation Sciences Program. We would like to thank the NASA WB-57F crew and management team for support during VIRGAS integration and flights. We thank E. Ray for flight planning during VIRGAS. The ACE mission is funded primarily by the Canadian Space Agency. Data from VIRGAS are available on a NASA online archive (https://www-air.larc.nasa.gov/missions/virgas/). Data from the MIPAS satellite are available at a KIT website (https://www.imk-asf.kit.edu/english/308.php). Data from the ACE-FTS satellite are available at a University of Waterloo website (http://www.ace.uwaterloo.ca/data.php).

References

Arfeuille, F., B. P. Luo, P. Heckendorn, D. Weisenstein, J. X. Sheng, E. Rozanov, M. Schraner, S. Brönnimann, L. W. Thomason, and T. Peter (2013), Modeling the stratospheric warming following the Mt. Pinatubo eruption: Uncertainties in aerosol extinctions, *Atmos. Chem. Phys.*, *13*(22), 11221–11234, doi:10.5194/acp-13-11221-2013.

Arnold, F., J. Curtius, S. Spreng, and T. Deshler (1998), Stratospheric aerosol sulfuric acid: First direct in situ measurements using a novel balloon-based mass spectrometer apparatus, *J. Atmos. Chem.*, *30*(1), 3–10, doi:10.1023/A:1006067511568.

Borrmann, S. et al. (2010), Aerosols in the tropical and subtropical UT/LS: In-situ measurements of submicron particle abundance and volatility, *Atmos. Chem. Phys.*, *10*(12), 5573–5592, doi:10.5194/acp-10-5573-2010.

Brühl, C., J. Lelieveld, P. J. Crutzen, and H. Tost (2012), The role of carbonyl sulphide as a source of stratospheric sulphate aerosol and its impact on climate, *Atmos. Chem. Phys.*, *12*(3), 1239–1253, doi:10.5194/acp-12-1239-2012.

Brühl, C., J. Lelieveld, H. Tost, M. Höpfner, and N. Glatthor (2015), Stratospheric sulfur and its

implications for radiative forcing simulated by the chemistry climate model EMAC, *J. Geophys. Res. Atmos.*, *120*(5), 2103–2118, doi:10.1002/2014JD022430.

Buchard, V., A. M. da Silva, P. R. Colarco, A. Darmenov, C. A. Randles, R. Govindaraju, O. Torres, J. Campbell, and R. Spurr (2015), Using the OMI aerosol index and absorption aerosol optical depth to evaluate the NASA MERRA Aerosol Reanalysis, *Atmos. Chem. Phys.*, *15*(10), 5743–5760, doi:10.5194/acp-15-5743-2015.

Chin, M., and D. D. Davis (1995), A reanalysis of carbonyl sulfide as a source of stratospheric background sulfur aerosol, *J. Geophys. Res.*, *100*(D5), 8993–9005, doi:10.1029/95JD00275.

Colarco, P., A. da Silva, M. Chin, and T. Diehl (2010), Online simulations of global aerosol distributions in the NASA GEOS-4 model and comparisons to satellite and ground-based aerosol optical depth, *J. Geophys. Res.*, *115*(D14), D14207, doi:10.1029/2009JD012820.

Crutzen, P. J. (1976), The possible importance of CSO for the sulfate layer of the stratosphere, *Geophys. Res. Lett.*, *3*(2), 73–76, doi:10.1029/GL003i002p00073.

Crutzen, P. J. (2006), Albedo Enhancement by Stratospheric Sulfur Injections: A Contribution to Resolve a Policy Dilemma?, *Clim. Change*, *77*(3–4), 211–220, doi:10.1007/s10584-006-9101-y.

Dentener, F. et al. (2006), Emissions of primary aerosol and precursor gases in the years 2000 and 1750, prescribed data-sets for AeroCom, *Atmos. Chem. Phys. Discuss.*, *6*(2), 2703–2763, doi:10.5194/acpd-6-2703-2006.

Doeringer, D., A. Eldering, C. D. Boone, G. Gonzlez Abad, and P. F. Bernath (2012), Observation of sulfate aerosols and SO2 from the Sarychev volcanic eruption using data from the Atmospheric Chemistry Experiment (ACE), *J. Geophys. Res. Atmos.*, *117*(3), 1–15, doi:10.1029/2011JD016556.

Duncan, B. N., S. E. Strahan, Y. Yoshida, S. D. Steenrod, and N. Livesey (2007), Model study of the cross-tropopause transport of biomass burning pollution, *Atmos. Chem. Phys.*, *7*(14), 3713–3736, doi:10.5194/acp-7-3713-2007.

Hofmann, D., J. Barnes, M. O'Neill, M. Trudeau, and R. Neely (2009), Increase in background stratospheric aerosol observed with lidar at Mauna Loa Observatory and Boulder, Colorado, *Geophys. Res. Lett.*, *36*(15), L15808, doi:10.1029/2009GL039008.

Höpfner, M. et al. (2013), Sulfur dioxide (SO2) as observed by MIPAS/Envisat: temporal development and spatial distribution at 15–45 km altitude, *Atmos. Chem. Phys.*, *13*(20), 10405–10423, doi:10.5194/acp-13-10405-2013.

Höpfner, M. et al. (2015), Sulfur dioxide (SO2) from MIPAS in the upper troposphere and lower stratosphere 2002–2012, *Atmos. Chem. Phys.*, *15*(12), 7017–7037, doi:10.5194/acp-15-7017-2015.

Junge, C. E., C. W. Chagnon, and J. E. Manson (1961), Stratospheric aerosols, *J. Meteorol.*,

18(1), 81–108, doi:10.1175/1520-0469(1961)018.

Kremser, S. et al. (2016), Stratospheric aerosol - Observations, processes, and impact on climate, *Rev. Geophys.*, *54*, 1–58, doi:10.1002/2015RG000511.

Marsh, D. R., M. J. Mills, D. E. Kinnison, J.-F. Lamarque, N. Calvo, and L. M. Polvani (2013), Climate Change from 1850 to 2005 Simulated in CESM1(WACCM), *J. Clim.*, *26*(19), 7372–7391, doi:10.1175/JCLI-D-12-00558.1.

McNutt, M. K. et al. (2015), *Climate Intervention: Reflecting Sunlight to Cool Earth*, Washington DC.

Mills, M. J. et al. (2016), Global volcanic aerosol properties derived from emissions, 1990-2014, using CESM1(WACCM), *J. Geophys. Res. Atmos.*, *121*(5), 2332–2348, doi:10.1002/2015JD024290.

Molod, A., L. Takacs, M. Suarez, and J. Bacmeister (2015), Development of the GEOS-5 atmospheric general circulation model: evolution from MERRA to MERRA2, *Geosci. Model Dev.*, *8*(5), 1339–1356, doi:10.5194/gmd-8-1339-2015.

Murphy, D. M., K. D. Froyd, J. P. Schwarz, and J. C. Wilson (2014), Observations of the chemical composition of stratospheric aerosol particles, *Q. J. R. Meteorol. Soc.*, *140*(681), 1269–1278, doi:10.1002/qj.2213.

Neely, R. R. et al. (2013), Recent anthropogenic increases in SO2 from Asia have minimal impact on stratospheric aerosol, *Geophys. Res. Lett.*, *40*(5), 999–1004, doi:10.1002/grl.50263.

Randel, W. J., M. Park, L. Emmons, D. Kinnison, P. Bernath, K. A. Walker, C. Boone, and H. Pumphrey (2010), Asian Monsoon Transport of Pollution to the Stratosphere, *Science*, *328*(5978), 611–613, doi:10.1126/science.1182274.

Rienecker, M. et al. (2007), The GEOS-5 Data Assimilation System--Documentation of Version 5.0.1, 5.1.0, and 5.2.0., *NASA Tech. Rep. Ser. Glob. Model. Data Assim.*, *27*, 1–118.

Rollins, A. W. et al. (2016), A laser-induced fluorescence instrument for aircraft measurements of sulfur dioxide in the upper troposphere and lower stratosphere, *Atmos. Meas. Tech.*, *9*(9), 4601–4613, doi:10.5194/amt-9-4601-2016.

Rosen, J. M. (1971), The Boiling Point of Stratospheric Aerosols, *J. Appl. Meteorol.*, *10*(5), 1044–1046, doi:10.1175/1520-0450(1971)010<1044:TBPOSA>2.0.CO;2.

Rosenlof, K. H., and J. R. Holton (1993), Estimates of the stratospheric residual circulation using the downward control principle, *J. Geophys. Res.*, *98*(D6), 10465–10479, doi:10.1029/93JD00392.

Schoeberl, M. R., A. R. Douglass, R. S. Stolarski, S. Pawson, S. E. Strahan, and W. Read (2008), Comparison of lower stratospheric tropical mean vertical velocities, *J. Geophys. Res.*,

390 *113*(D24), D24109, doi:10.1029/2008JD010221.

391 Sheng, J. X., D. K. Weisenstein, B. P. Luo, E. Rozanov, A. Stenke, J. Anet, H. Bingemer, and T.
392 Peter (2015), Global atmospheric sulfur budget under volcanically quiescent conditions:
393 Aerosol-chemistry-climate model predictions and validation, *J. Geophys. Res. Atmos.*,
394 *120*(1), 256–276, doi:10.1002/2014JD021985.

395 Shepherd, J. G. (2012), Geoengineering the climate: an overview and update., *Philos. Trans. A.*
396 *Math. Phys. Eng. Sci.*, *370*(1974), 4166–75, doi:10.1098/rsta.2012.0186.

397 Smith, S. J., J. Van Aardenne, Z. Klimont, R. J. Andres, A. Volke, and S. Delgado Arias (2011),
398 Anthropogenic sulfur dioxide emissions: 1850-2005, *Atmos. Chem. Phys.*, *11*(3), 1101–
399 1116, doi:10.5194/acp-11-1101-2011.

400 Solomon, S. (1999), Stratospheric ozone depletion: A review of concepts and history, *Rev.*
401 *Geophys.*, *37*(3), 275–316, doi:10.1029/1999RG900008.

402 Stenke, A., M. Schraner, E. Rozanov, T. Egorova, B. Luo, and T. Peter (2013), The SOCOL
403 version 3.0 chemistry-climate model: Description, evaluation, and implications from an
404 advanced transport algorithm, *Geosci. Model Dev.*, *6*(5), 1407–1427, doi:10.5194/gmd-6-
405 1407-2013.

406 Strahan, S. E., B. N. Duncan, and P. Hoor (2007), Observationally derived transport diagnostics
407 for the lowermost stratosphere and their application to the GMI chemistry and transport
408 model, *Atmos. Chem. Phys.*, *7*(9), 2435–2445, doi:10.5194/acp-7-2435-2007.

409 Thomason, L., and T. Peter (2006), *Assessment of stratospheric aerosol properties (ASAP)*.

410 Vernier, J. P. et al. (2011), Major influence of tropical volcanic eruptions on the stratospheric
411 aerosol layer during the last decade, *Geophys. Res. Lett.*, *38*(12), 1–8,
412 doi:10.1029/2011GL047563.

413 Yu, P., D. M. Murphy, R. W. Portmann, O. B. Toon, K. D. Froyd, A. W. Rollins, R. Gao, and K.
414 H. Rosenlof (2016), Radiative forcing from anthropogenic sulfur and organic emissions
415 reaching the stratosphere, *Geophys. Res. Lett.*, *43*(17), 9361–9367,
416 doi:10.1002/2016GL070153.

417
418

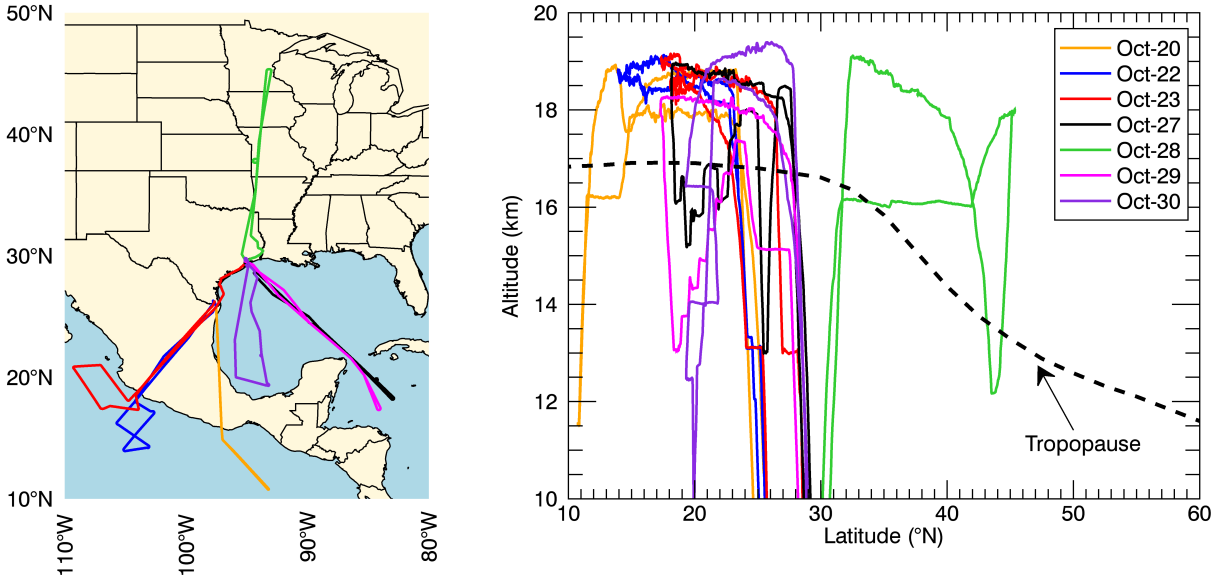

419

420 **Figure 1**. Flight tracks from the VIRGAS experiment during October 2015.

421

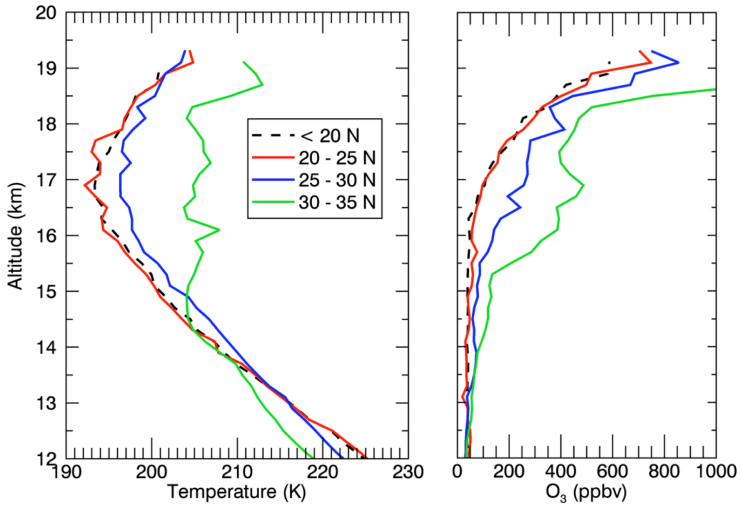

422

423 **Figure 2**. Mean temperature (left) and ozone (O_3, right) profiles for four latitude ranges sampled
424 during VIRGAS. Similarities of temperature and O_3 from 10 - 25 °N suggest data up to 25
425 °N are representative of tropical air masses on these flights.

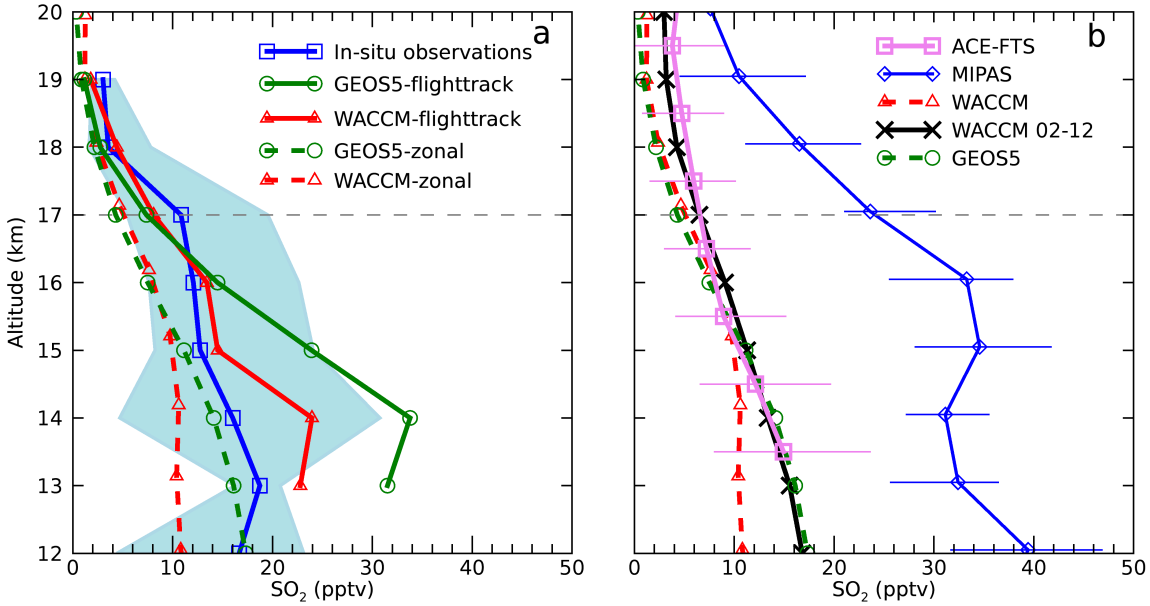

Figure 3. Measured and modeled SO_2 profiles in the tropical (10 - 25 °N) UT/LS. (a) Blue line and shaded region show the VIRGAS in-situ measurement median and interquartile range. WACCM and GEOS-5 have been adjusted upwards by 1 km to match the aircraft ozone and thermal tropopause level. Two profiles each are shown for WACCM and GEOS-5: one for the zonal mean for 2015 (dash lines), and another showing data sampled from the models along the flight track locations / times (solid lines). (b) ACE-FTS median and interquartile range (2004-2010). MIPAS median and interquartile range of monthly means (2002 – 2012). Data during periods affected by major volcanic events were omitted from the ACE-FTS and MIPAS data [*Höpfner et al.*, 2013]. WACCM and GEOS-5 profiles are the same zonal mean profiles shown in panel (a). WACCM 02-12 profile (black) shows the mean profile obtained by sampling the WACCM run during the 2002 – 2012 MIPAS period [*Mills et al.*, 2016], from the same times and locations as the MIPAS data that are averaged to derive the blue MIPAS profile.